Brownian Dynamics Simulations of the Reactions of Hydrated Electrons with Components of DNAs and a DNA Double-Helix

ARNAUD J. A. SOIRAT, CHUNG F. WONG, ROMAN OSMAN, HAREL WEINSTEIN

Department of Physiology and Biophysics, Mount Sinai School of Medicine of The City University of New York, New York, New York 10029

Received 3 July 1996; accepted 25 September 1996

ABSTRACT: As a first step toward developing simulation models for studying the indirect mechanism of radiation damage to DNAs, we have carried out Brownian dynamics simulations to study the reactions of hydrated electrons with a 12-base-pair B-DNA, $(dA)_{12}(dT)_{12}$, and with bases, monodeoxynucleotides, and polydeoxynucleotides. We first studied in detail the sensitivity of diffusion reaction rate constants to different model and simulation parameters. Based on the sensitivity studies, a set of model and simulation parameters was obtained for the final production runs. The use of this set of parameters reduced the computational costs but delivered reasonably reliable results. The calculated reaction rate constants were in qualitative agreement with experiments. For the DNA double-helix, $(dA)_{12}(dT)_{12}$, the simulations demonstrated that hydrated electrons preferred to attack the two ends of the double-helix. Electrostatic interactions between the DNA and the hydrated electrons make the T strand more susceptible to attack than the A strand. The increased reactivity of the T strand due to electrostatic interactions results from the increased reactivity of the C6 sites of the thymine bases, at the expense of the reactivity of the C8 sites of the adenine bases. The reactivity of the relatively buried reactive sites of the adenine and thymine bases are less affected by electrostatic interactions.
 J Comput Chem **18:** 888–901, 1997

Keywords: Brownian dynamics simulations; sensitivity analysis; radiation damage to DNAs; hydrated electron

Correspondence to: C. F. Wong; e-mail: wong@msvax.mssm.edu

Contract grant sponsor: Petroleum Research Fund of the American Chemical Society

Contract grant sponsor: The National Institutes of Health

Contract grant sponsor: The Department of Energy

 CCC 0192-8651 / 97 / 070888-14

Introduction

When a living body is exposed to high-energy radiation, most of the cell deaths are caused by DNA damage. DNA molecules are damaged either by direct interaction with radiation, or indirectly through radicals or hydrated electrons generated in the surroundings of DNAs by the radiation[1]. If the damaged DNAs are not repaired, cell death will result.

In aqueous cell media, water is decomposed by radiation into primary reactive species such as hydrated electrons, OH radicals, and H radicals[2]. These species diffuse to and damage DNAs. In aqueous solutions, the bases of DNA molecules are attacked mainly by hydrated electrons, H radicals, and OH radicals through addition reactions. The sugars, on the other hand, are attacked by hydroxyl radicals through hydrogen abstractions [3–6].

Consideraable experimental and theoretical efforts have been made to elucidate the molecular mechanism of DNA damage induced by high energy radiation[1,3,7]. In this article, we study the indirect mechanism of radiation damage to DNAs. In particular, we have used the technique of Brownian dynamics simulation[8,9] to elucidate how hydrated electrons generated from water by radiation diffuse to and attack DNA molecules. In contrast to previous theoretical works, the simulation models employed here are more realistic by taking into account the detailed electrostatic interactions between hydrated electrons and DNAs. The ultimate goal is to integrate dynamic simulations with quantum chemical methods to obtain a detailed microscopic understanding of how hydroxyl and hydrogen radicals attack DNAs. These radicals are responsible for most of the strand breaks in the indirect mechanism of radiation damage[10,11]. Quantum chemical methods have already been used to estimate the activation barriers for the abstraction of hydrogens from the sugar moieties of DNAs by hydroxyl radicals[12]. The purpose of the Brownian dynamics simulations presented here is to develop and evaluate simulation models that can be integrated with results from quantum chemical calculations to quantify the rate constants of the reaction of hydroxyl and hydrogen radicals with DNAs, and to predict the probability that these radicals attack different sites of the DNAs.

The study of the reactions of hydrated electrons with DNAs and components of DNAs serves as a useful first step for setting up and testing Brownian dynamics simulation models for studying the indirect mechanism of radiation damage to DNAs. This is because these reactions are diffusion-controlled,[13] so that every collision between a hydrated electron and a reactive site on a DNA molecule can be considered as a successful reaction. This makes the Brownian dynamics simulation model simpler. On the other hand, the attack of the sugar moieties and the bases by the hydroxyl radicals are not likely to be strictly diffusion-limited[13], as also suggested by quantum calculations[12] that the activation barriers for the addition of radicals to the bases and the hydrogen abstraction from the sugars by the radicals are non-negligible. A proper theoretical understanding and prediction of the reaction rate constants will therefore require an integrated study of both the relative diffusion between DNAs and DNA-damaging agents, and the subsequent reactions that take place. The simulation models are somewhat more complicated because one has to take into account the fact that not every collision between a radical and a reactive site on a DNA results in a reaction. It is therefore useful to first demonstrate that a simpler simulation model of the diffusion encounter between hydrated electrons and DNAs or their components can give reliable results before more complex models are constructed for studying the reactions between OH or H radicals and DNAs.

In this article, we present results of the use of the Ermak–McCammon algorithm[8] for carrying out Brownian dynamics simulations. The reaction rate constant between hydrated electrons and $(dA)_{12}(dT)_{12}$ or components of DNAs was calculated by assuming that the reaction was diffusion-controlled. The relative probabilities of attack of different reactive sites on a $(dA)_{12}(dT)_{12}$ double-helix by hydrated electrons were also predicted.

Methods

Brownian dynamics simulations have been carried out using the algorithm developed by Ermak and McCammon[8]. The calculations of the reaction rates were based on the method of Northrup et al[14]. The interaction force between a hydrated electron and a DNA double-helix or a fragment of DNA was calculated by multiplying the charge of the hydrated electron to the electrostatic field

around the DNA double-helix or the DNA fragment. The electrostatic field around a molecule was calculated by solving the linearized Poisson–Botzmann equation (LPBE)[15–22]. The algorithm for carrying out these calculations have been implemented in the UHBD program (version 1.0)[23]. We have modified the program to use variable time steps, to estimate statistical errors of diffusion reaction rate constants, and to study the relative probability of attack of different sites of a DNA molecule by hydrated electrons. Hydrodynamic interactions were neglected in all the calculations presented in this article.

In the simulations, we fixed target molecule [bases, monodeoxynucleotides, polydeoxynucleotides, or $(dA)_{12}(dT)_{12}$] at the origin, and let the hydrated electron diffuses around the target molecule with a diffusion constant equal to the sum of the diffusion constants of the hydrated electron and the target molecule. The electrostatic field around the target molecule was calculated by solving the Poisson–Boltzmann equation (PBE). The solution of the PBE was carried out by dividing the Cartesian space into two regions: an inner region with low dielectric constant, and an outer region with high dielectric constant. The boundary between the inner region and outer region was defined by the shape of the target molecule. The shape of the target molecule was defined by using the van der Waals radii of the atoms in the target molecule.

The PBE could be given by:

$$-\nabla \cdot (\varepsilon(\mathbf{r})\nabla\phi(\mathbf{r})) = \rho(\mathbf{r}) - en_\infty \sinh\left(\frac{e\phi(\mathbf{r})}{k_bT}\right) \quad (1)$$

where $\varepsilon(\mathbf{r})$ is the dielectric function, $\phi(\mathbf{r})$ is the electrostatic potential evaluated at $\mathbf{r}$, $\rho(\mathbf{r})$ is the charge density, e is the electronic charge, n_∞ is the number density of ions, k_b is the Boltzmann constant, and T is the absolute temperature.

To make it easier to solve eq. (1), the PBE is usually linearized to give:

$$-\nabla \cdot (\varepsilon(\mathbf{r})\nabla\phi(\mathbf{r})) + \varepsilon(\mathbf{r})\kappa^2\phi(\mathbf{r}) = \rho(\mathbf{r}) \quad (2)$$

where κ is the inverse Debye–Hückel screening length, given by:

$$\kappa^2 = \frac{Ie^2}{k_bT\varepsilon} \quad (3)$$

where i is the ionic strength.

Although analytical solutions to the PBE are possible for molecules of simple shape, numerical solutions of the PBE are required for molecules of complex shape and characteristics of biomolecules. Different numerical techniques have been developed for solving the LPBE. The algorithm in the UHBD program is based on the finite-difference method[15]. The basic idea of the finite-difference method is to transform the partial differential equation [eq. (2)] into a set of linear equations, by discretizing space into cubic grids and approximating the derivatives by finite differences.

Once the potential $\phi(\mathbf{r})$ around the static molecule was obtained, the force, $\mathbf{F}(\mathbf{r})$, acting on the moving molecule was calculated by the test charge method. In the test charge method, the effects of solvent exclusion volume of the diffusing molecule and reaction field were ignored. This was a reasonable approximation in these calculations because the diffusing species, hydrated electron, was much smaller than the target molecule.

The trajectory of a diffusing particle could be simulated by using the Ermak–McCammon algorithm[8];

$$\mathbf{r} = \mathbf{r}_O + \frac{1}{k_bT}D\mathbf{F}(\mathbf{r}_O)\Delta t + \mathbf{R} \quad (4)$$

where $\mathbf{r}$ is the new position vector obtained after a dynamics time step of Δt, D is the relative diffusion constant which was approximated by the sum of the diffusion constants of the hydrated electron and the target molecule, $\mathbf{F}(\mathbf{r}_O)$ is the force acting on the diffusing particle at $\mathbf{r}_O$ (calculated from the electrostatic potential at $\mathbf{r}_O$ using the test charge method), and $\mathbf{R}$ is a Gaussian random displacement with a mean of zero and a variance of:

$$\langle \mathbf{R}^2 \rangle = 2D\Delta t \quad (6)$$

This random displacement was the result of the random collisions of solvent molecules with the diffusing molecules.

In the calculations, the hydrated electron was placed at random on the surface of a sphere (b surface defined by the parameter b_{surf}) which divided the Cartesian space into an inner and an outer region. The b value was chosen such that the electrostatic potential was centrosymmetric for $r > b$. The trajectory of the diffusing particle was simulated by the Ermak-McCammon algorithm[8] and the trajectory was terminated when one of the

following conditions was satisfied:

1. The trajectory moved far away from the target and crossed another surface defined by a sphere with radius q (q surface characterized by the parameter q_{surf} where $q > b$.
2. The trajectory came close to and reacted with one of the reactive centers of the target molecule.

By running a large number of trajectories, one could obtain a probability, β, that a diffusing molecule started at the b surface reacted with the target molecule rather than diffused to the q surface. β could be used to calculate another probability, P; that is, the probability of a diffusing molecule starting at the b surface that would react with the target molecule rather than diffuse to infinity. The biomolecular diffusion-controlled rate constant, k, could then be obtained from[14]:

$$k = k_D(b)P \tag{7}$$

where $k_D(b)$ is the rate constant for the two species to come to a separating distance of b. Because b was chosen such that the electrostatic potential, $\phi(\mathbf{r})$, was centrosymmetric for $r \geq b$, $k_D(b)$ could be calculated from[24]:

$$k_D(b) = \frac{4\pi}{\int_b^\infty \frac{e^{[\phi(\mathbf{r})/k_bT]}}{r^2D}\,\mathrm{d}r} \tag{8}$$

The probability P could be expressed as[14]:

$$P = \frac{\beta}{1 - (1 - \beta)\Omega} \tag{9}$$

where Ω is given by:

$$\Omega = \frac{k_D(b)}{k_D(q)} \tag{10}$$

This formulation of the rate constant is valid when every collision of the diffusing particle with a reaction center of the target molecule leads to a reaction; that is, when the reaction is diffusion-controlled.

We have modified the UHBD program[23] to use variable time steps so that simulation time could be reduced. The use of the variable time-step algorithm decreased the computational time by about an order of magnitude relative to a constant time-step algorithm. In the variable time-step algorithm, the space $r < q$ was divided into four regions ($r = p < b < c < q$):

1. $r \leq p$ region: the time step, Δt, was at its minimum constant value of Δt(min).
2. $p < r \leq b$ region: the time step varied from its minimum value to its maximum one, Δt(max) at $r = b$, by:

$$\Delta t = a_1\, r^{n_1} + b_1 \tag{11}$$

where the constants a_1 and b_1 are given by:

$$a_1 = \frac{(\Delta t(\max) - \Delta t(\max))}{(b^{n_1} - p^{n_1})} \tag{12}$$

and:

$$b_1 = \Delta t(\max) - a_1\, b^{n_1} \tag{13}$$

3. $b < r \leq c$ region: the time step was at its maximum value Δt(max) and was constant.
4. $c < r \leq q$ region: the time step varied from its maximum value to its minimum one according to:

$$\Delta t = a_2 r^{n_2} + b_2 \tag{14}$$

where the constants a_2 and b_2, are given by:

$$a_2 = \frac{(\Delta t(\max) - \Delta(\min))}{\left(c_{n_2} - q^{n_2}\right)} \tag{15}$$

$$b_2 = \Delta t(\max) - a_2\, c^{n_2} \tag{16}$$

and n_2 was an integer.

Construction of Models, Choice of Model and Simulation Parameters, and Sensitivity of Simulation Results to the Choice of Model Parameters

Brownian dynamics simulations have been carried out to study the reaction of hydrated electrons with DNAs and their constituents including:

1. Free bases: adenine (Ade), guanine (Gua), cytosine (Cyt), thymine (Thy), and uracil (Ura).
2. 5′-Deoxynucleotides: 5′dAMP, 5′dGMP, 5′-dCMP, and 5′-dTMP.
3. A single-stranded 5′-polydeoxynucleotide: 5′-$(dA)_6$.
4. A double-stranded B-DNA: $(dA)_{12}(dT)_{12}$.

The three-dimensional structures of these molecules were generated by using the QUANTA program[25]. The Van der Waals atomic radii were those of CHARMM[26].

In the next section, we report the values of the model and simulation parameters used in the Brownian dynamics simulations. Due to the lack of experimental data, there were uncertainties in choosing some of the model parameters, and therefore we have spent some time examining the sensitivity of the simulated rate constants to the choice of the model parameters. The sensitivity analysis had also helped to ''optimize'' some simulation parameters for reducing the amount of computational time for the final production runs.

ELECTRONIC PARAMETERS

Charge Table

In calculating the electrostatic field around the bases, monodeoxnucleotides, polydeoxynucleotide, and the DNA molecule, the AMBER[27] charges were used in the solution of the Poisson–Boltzmann equation. These charges were originally derived by requiring them to reproduce as closely as possible the electrostatic potentials around components of DNA molecules. The electrostatic potentials were obtained by carrying out *ab initio* calculations using the STO3G basis set. As shown later, the use of the AMBER charges gave reactive rate constants comparable to experimental ones.

Ionic Strength

In all calculations, the ionic strength was kept at the commonly used experimental value of 100 mM, allowing easier comparisons with experimental results.

Grid Parameters

In the UHBD program[23], the Poisson–Boltzmann equation is solved by using the finite-difference method in which a finite region of space containing a molecule is represented by a cubic grid. Two parameters characterize the grid used to calculate the potentials around a molecule: h, the grid spacing, and n_{grid}, the number of grid points in each direction of space.

The choice of n_{grid} is directly related to that of h. For a given choice of h, n_{grid} should be chosen large enough so that the whole grid completely encloses the molecule around which the electrostatic potentials are to be calculated. To use eq. (7)–(10) to calculate the reactive rate constants, the grid should also be large enough so that the electrostatic potential around the molecule is centrosymmetric near the boundary of the grid. However, hardware considerations usually limit the maximum value of n_{grid} that can be used in the calculations. For example, $n_{\text{grid}} = 120$ was the maximum reasonable value that we could use on a Silicon Graphics 4D/260S with 128 Mb of RAM without degrading the performance of the machine due to excessive paging. Therefore, for large molecules, such as proteins or DNAs, one has to sacrifice some accuracies in solving the LPBE by using somewhat larger values of h. Due to these limitations, we have done some calculations to investigate the influence of the choice of h and n_{grid} on the computed rate constant for the reaction between hydrated electrons and the base adenine (Table I).

The results from Table I show that: (1) at constant h, the calculated k is insensitive to the choice of n_{grid} as long as the grid is large enough to enclose the target molecule and gives a centrosymmetric potential near its boundary; and (2) k is more sensitive to the choice of h, although k does not vary dramatically for a given constant grid volume.

TABLE I.
Sensitivity of the Rate Constant k on Choice of h and n_{grid} for Reaction Between Ade and Hydrated e^-.

h (Å)	n_{grid}	Volume (Å^3)	β	k ($10^9 M^{-1}s^{-1}$)
0.7	80	56	0.04475	12.4 ± 1.6
0.7	114	80	0.04462	12.3 ± 0.7
1.0	80	80	0.04787	13.2 ± 1.9
0.5	112	56	0.03800	10.5 ± 0.8

Eight batches of 1000 (n_{traj} = 8x1000) trajectories were run for each choice of h and n_{grid}. A rate constant was obtained from each batch of trajectories. The average result from the eight batches is reported. The error bars are estimated from the standard deviation of the results obtained from the eight batches. h_{r1} = 4.0 Å, h_{r2} = 0.5 Å, p_{surf} = 20 Å, b_{surf} = 50 Å, q_{surf} = 200 Å, Δt(min) = 0.2 ps. h_r is the hydrodynamic radius of the target molecule, which is an adenine base in this case. h_{r2} is the hydrodynamic radius chosen to give a diffusion coefficient of an electron equal to the experimental value. p_{surf} defines a p surface within which reaction criteria are checked. The p surface is also a parameter in the variable time-step algorithm.

TABLE II.
Sensitivity of k on Choice of h for the Reaction Between Hydrated Electrons and $(dA)_{12}(dT)_{12}$.

h (Å)	n_{grid}	β	k ($10^9 M^{-1}s^{-1}$)
2.5	120	0.00015	0.270 ± 0.005
4.0	120	0.00012	0.228 ≡ 0.006

Rate constants and β values are given per nucleotide base. h_{r1} = 19.0 Å, h_{r2} = 0.5 Å, p_{surf} = 60 Å, b_{surf} = 120 Å, c_{surf} = 140 Å, q_{surf} = 160 Å, Δt(min) = 0.1 ps, Δt(max) = 7.3 ps, n_1 = 1.5, n_2 = 1.0, and n_{traj} = 4 x 10,000.

For a larger and highly charged DNA molecule, it is necessary to use a larger grid. However, due to hardware limitations, we were forced to use a relatively large grid spacing h of 2.5 Å. For n_{grid} = 120, a grid volume of 300 Å^3 resulted. Because the grid spacing was large, we have examined the reliability of the calculations by evaluating k using two sets of grid parameters. In set 1, h = 2.5 Å and n_{grid} = 120. In set 2, h = 4.0 Å and n_{grid} = 120. The results are summarized in Table II. It appears from Table II that the uncertainty of k due to the choice of grid spacing is $\sim 20\%$.

Although it was probably more accurate to solve the full, instead of the linearized, PBE in obtaining the electrostatic potential around a DNA molecule, the linear approximation had been shown to give reasonable transport properties of DNAs in concentrated DNA solutions at ionic strengths similar to the one used here[28]. The qualitative trends of the simulated reaction rate constants and the insights into the preferred sites of attack by hydrated electrons should not be affected by this approximation. Moreover, the effects of removing the linear approximation might be estimated. In a recent study[29], a Brownian dynamics simulation model —which did not use the linear approximation and accounted for finite ion size effects—had been used to study ion-pair distributions in ionic solutions. When comparing the results obtained from these simulations with those from linearized Poisson–Boltzmann theory, it appeared that the consequence of using the linear approximation was the overscreening of charge interactions. Therefore, the reactive rate constants obtained using the linearized approximation would be overestimated because the repulsion between the hydrated electrons and the negatively charged DNA was underestimated. Although the current simulation model can be further improved, it is already much more sophisticated than previous models employed in studying DNA damage by hydrated electrons. For example, electrostatic interactions between hydrated electrons and DNAs have been ignored in previous models.

BROWNIAN DYNAMICS SIMULATION PARAMETERS

We have also examined the sensitivity of the calculated reaction rate constants to the choice of parameters that are related to the solution of the diffusion equation and the calculation of reaction rate constants. The results are summarized next.

Reaction Centers

Many studies have been published on using experimental methods to determine the sites of DNA molecules that are attacked by hydrated electrons, although there are still contradictory conclusions from the experimental data. It is now accepted that hydrated electrons react only with the bases of DNA molecules. However, the precise sites of their attacks are still the subject of debate. For example, attacks on C2 and C4 of pyrimidine bases by hydrated electrons have been observed by Hayon[30]. Others, however, ruled out this possibility and claimed to have observed an exclusive C5—C6 reactivity[4, 31–33]. The purine reactivity with hydrated electrons is less documented and a C8 attack has been reported[5].

Because the experimental data are somewhat inconclusive regarding the sites of attack by hydrated electrons, we have included all the reported sites of attack (Table III) as possible reactive sites in the Brownian dynamics simulations. An electron was assumed to have reacted with a reactive site on a base if it reached a distance less that 1.9 Å from the reactive site. If an electron hit a nonreactive site on the DNA, this move was rejected. Because the choice of reactive centers on the bases was somewhat arbitrary, due to inconclusive experimental findings, we examined the sensitivity of the reaction rate constants to the choice of reac-

TABLE III.
Reaction Centers on a DNA Molecule.

Pyrimidine bases	C2, C4, C5, C6
Purine bases	C2, C4, C5, C6, C8
Sugar moieties	none

TABLE IV.
Sensitivity of Reaction Rate Constant *k* on the Choice of Reactive Centers for the Reaction of Hydrated Electrons with Ade and Cyt.

Molecule	Reaction centers	β	k ($\times 10^9 M^{-1}s^{-1}$)
Ade	C8	0.01595	11.10 ± 0.03
	C4, C5, C8	0.01850	12.8 ± 0.8
	C2, C4, C5, C6 C8	0.01830	12.7 ± 0.2
Cyt	C2, C4	0.01145	8.3 ± 0.5
	C5, C6	0.01340	9.6 ± 0.6
	C2, C4, C5, C6	0.01375	9.9 ± 0.9

h_{r1} (Ade) = 4.0 Å, h_{r1}(Cyt) = 3.0 Å, h_{r2} = 0.5 Å, p_{surf} = 20 Å, b_{surf} = 100 Å, c_{surf} = 200 Å, q_{surf} = 250 Å, Δt(min) = 0.1 ps, Δt(max) = 40.0 ps, n_1 = 1.0, n_2 = 1.0, and n_{traj} = 2 x 10,000.

tive centers. Table IV summarizes the results, which show that the rate constants are somewhat sensitive to the choice of reactive centers, but the variations among the rate constants obtained by using different sets of reactive sites are less than 10%.

Hydrodynamic Radii

In the BD simulations, estimates of the diffusion coefficients of the molecules studied are required. We used experimental values whenever they were available. When the experimental hydrodynamic radius, r_h, of a molecule was known, the diffusion coefficient of the molecule was obtained using the Stokes–Einstein relation:

$$D = \frac{k_b T}{6\pi\eta r_h} \tag{17}$$

where η is the viscosity of water. If experimental data were not found, the hydrodynamic radii were estimated from the geometric size of the molecules.

For the hydrated electron, the experimental value of the diffusion coefficient was $4.9 \cdot 10^{-5}$ cm^2/s[34]. The hydriodynamic radii of the target molecules were fixed at the values given in Table V. The r_h values of the bases and the deoxy nucleotides were estimated according to the work of Bowen et al[35]. The DNA r_h value was estimated by using a theoretical method developed by Garcia de al Torre and coworkers for short DNA fragments[36].

For large molecules, one does not expect k to be very sensitive to the choice of r_h because they diffuse much slower than a hydrated electron. The relative diffusion coefficient of a large molecule and a hydrated electron, which can be approximated by the sum of the diffusion coefficients of the molecule and the hydrated electron when hydrodynamic interactions are neglected, is very similar to that of a hydrated electron. On the other hand, small molecules such as bases have diffusion constants that are comparable to that of a hydrated electron. A small change in r_h of a small molecule may thus give a somewhat different value for the relative diffusion coefficient between the molecule and the hydrated electron, which in turn may give a somewhat different value for k. We have therefore checked the sensitivity of the rate constant for the reaction between hydrated electrons and one of the bases, adenine, to the choice of r_h. The results are shown in Table VI, which suggest that the reaction rate constant is not too sensitive to the uncertainty of the hydrodynamic radius of the adenine base. Decreasing r_h of the adenine base by a factor of 2 only changes the reaction rate constant by $\sim 4\%$.

Time Steps

A variable time-step algorithm, as described earlier, was used. This algorithm substantially saves computational time. The main reason for using a distance-dependent time step was that it allowed a diffusing hydrated electron to make big

TABLE V.
Hydrodynamic radii (in Å) Used in the Brownian Dynamics Simulations.

Bases		Deoxynucleotides			
Purines	Pyrimidines	Purines	Pyrimidines	5′-$(dA)_6$	B-DNA(12 base pairs)
4	3	6	6	10	19

TABLE VI.
Sensitivity of *k* on the Choice of Hydrodynamic Radius for the Reaction Between Hydrated *e* and Adenine.

r_h (in Å)	2	4
β	0.01725	0.01830
$k(\times 10^9 M^{-1}s^{-1})$	13.3 ± 0.1	12.7 ± 0.2

h = 1.4 Å, n_{grid} = 120, h_{r2} = 0.5 Å, p_{surf} = 20 Å, b_{surf} = 100 Å, c_{surf} = 200 Å, q_{surf} = 250 Å, Δt(min) = 0.1 ps, Δt(max) = 40.0 ps, n_1 = 1.0, n_2 = 1.0, and n_{traj} = 2 x 10,000.

''jumps'' in regions far away from the target molecule. In such distant regions, the electrostatic forces between the hydrated electron and the target molecule were negligible and the relative diffusion was nearly random and followed Gaussian statistics. On the other hand, small time steps were used when the hydrated electron was very close to the target molecule so that the electrostatic interactions were relatively large and rapidly changing, requiring the use of small time steps in the Ermak–McCammon algorithm[8]. To facilitate the choice of the minimum and maximum time steps in the production runs, we performed the following analysis.

Consider a jump between two consecutive steps in a Brownian dynamics simulation. According to the Einstein formula for a spherical object undergoing a Brownian motion in a three-dimensional space, the root mean square displacement λ between two consecutive steps is given by:

$$\lambda = (6D\Delta t)^{1/2} \tag{18}$$

Applying this formula with D is equal to the sum of the diffusion constants of a hydrated electron and a polydeoxynucleotide $(dA)_6$ and, if Δt = 0.1 ps and 100 ps, one gets λ = 0.5 Å and 17 Å, respectively. Therefore, 0.1 ps appears to be a reasonable minimum time step to use because λ is small relative to the separations of the reactive sites. a maximum time step of 100 ps is also reasonable to use in the region $b < r \leq c$ because b is usually chosen to be larger than 17 Å. However, this formula is only valid when the interaction forces are zero. To obtain a more realistic picture of the relative diffusion of a hydrated electron and a $(dA)_6$, we recorded the magnitude of each jump occurring in a Brownian dynamics simulation. For Δt = 100 ps, jumps as large as ~ 100 Å could occur during the simulation. Although these jumps rarely occurred and the maximum time step was only used in the region $b < r \leq c$, we decided to be more cautious and chose a maximum time step of 40 ps. The use of a minimum time step of 0.1 ps in the region close to the target [$r < 35$ Å for the $(dA)_6$] generated maximum jumps of ~ 1.2 Å. The mean displacement in this region was found to be very close to the estimate of 0.5 Å by using the Einstein formula. These jumps were reasonably small even for determining the relative probabilities of attack of different sites on a DNA double-helix by hydrated electrons.

The *p*, *b*, *c*, and *q* Surfaces

As mentioned earlier, the b surface has to be chosen far enough from the target molecule so that the electrostatic potential is centrosymmetric outside the b surface. Once this condition is satisfied, the choice of the c and q surfaces are somewhat arbitrary, although their choices are related to the choice of time steps. As a rule of thumb, one should choose a q surface and a time step such that, whenever a trajectory is terminated because it jumps outside the q surface, the trajectory should end at a point as close to the q surface as possible. We have carried out simulations to verify the insensitivity of k to the choice of the b, c, and q surfaces and the results are presented in Table VII. Because the variation of time steps in the variable time-step algorithm depends on the choice of the surfaces, the curvatures of the time-step–distance functions were chosen such that the variations of time steps for all the simulations were about the same for $r \leq 90$ Å.

The same kind of analysis had been performed when no electrostatic forces were felt by the diffusing hydrated e^-. Approximately the same Δt variations in the region between the p and b surfaces were maintained by suitably changing Δt(max) for

TABLE VII.
Sensitivity of *k* on the Choice of Surface Parameters for the Reaction Between Hydrated Electrons, and 5′-$(dA)_6$.

b_{surf} (Å)	c_{surf} (Å)	q_{surf} (Å)	β	k ($10^9 M^{-1}s^{-1}$)
300	400	450	0.00036	1.26 ± 0.05
300	600	650	0.00058	1.27 ± 0.00
500	600	650	0.00016	1.34 ± 0.02

Rate constants and β values are given per nucleotide base. h = 2.5 Å, n_{grid} = 120, Δt(min) = 0.1 ps, Δt(max) = 40.0ps, h_{r1} = 10.0 Å, p_{surf} = 40.0 Å, n_1 (b_{surf} = 300) = 1.5, n_1 (b_{surf} = 500) = 1.0, n_2 = 1.0, n_{traj} (first and third tests) = 2 x 10,000, and n_{traf} (second test) = 1 x 10,000.

TABLE VIII.
Sensitivity of k on the Choice of the Surface Parameters for the Reaction Between Hydrated Electron and 5′-$(dA)_6$ (No Electrostatic Force).

Δt(max) (ps)	b_{surf} (Å)	c_{surf} (Å)	q_{surf} (Å)	β β	k (no f) ($10^9 M^{-1}s^{-1}$)
40	300	400	450	0.00106	3.70 ± 0.02
12.9	150	200	225	0.00215	3.69 ± 0.07
6.15	100	120	140	0.00288	3.78 ± 0.02

Rate constants and β values are given per nucleotide base. h = 1.5 Å, n_{grid} = 30, Δt(min) = 0.1 ps, p_{surf} = 40.0 Å, h_{r1} = 10.0 Å, n_1 = 1.5, n_2 = 1.0, and n_{traj} = 4 x 50,000.

a given choice of the b surface instead of changing the curvature of the time-step–distance function. For such a pure random motion, Table VIII shows that k is virtually insensitive to the choice of surface parameters.

Summary

To summarize, the sensitivity analysis of the different model parameters on k, performed for the bases, deoxynucleotides, $(dA)_6$, and the 12-base-pair B-DNA has shown that:

1. For the electrostatic parameters, k was only slightly sensitive to the choice of grid spacing.
2. In the Brownian dynamics simulations, k was somewhat sensitive to the set of atoms chosen as reaction centers. Because the experimental determination of the reaction centers were still ambiguous, our choices of reaction centers in the simulations were also somewhat uncertain. However, the rate constant varied by less than 10% when different sets of reaction sites were chosen.
3. It was also shown that the choice of the hydrodynamic radii of the large DNA molecule was not crucial because its diffusion coefficient was much smaller than that of a hydrated electron.
4. The choice of time steps and b, c and q surfaces was based on the compromise between two factors. One was a strong desire to minimize the cpu time required for completing simulation, which translated into the use of high Δt's and choices of the b, c, and q surfaces close to the target molecule. The other was the requirement to use a large enough b values so that the electrostatic potential was centrosymmetric outside the b surface, and small enough Δt values so that the Ermak–McCammon algorithm[8] could be solved accurately and the conditions for terminating trajectories could be determined reliably. The test calculations presented generated a set of simulation parameters to use in the final production runs. These parameters had reduced simulation time but delivered reasonably reliable results for the rate constants.

Based on the sensitivity analysis of the different model and simulation parameters on the various rate constants, we had come up with the parameters for the production runs listed in Table IX.

Rate Constants for Attack of Bases, Deoxynucleotides, $(dA)_6$, and $(dA)_{12}(dT)_{12}$ by Hydrated Electrons

Using the model and simulation parameters presented in Table IX, the rate constants for the attack of bases, monodeoxynucleotides, $(dA)_6$, and $(dA)_{12}(dT)_{12}$ by hydrated electrons were calculated. The results are reported in Table X, together with the available experimental results.

TABLE IX.
Model and Simulation Parameters Used in the Production Runs.

System	h (Å)	Grid pts.	h_{r1} (Å)	p_{surf} (Å)	b_{surf} (Å)	c_{surf} (Å)	q_{surf} (Å)	Δt(min) (ps)	Δt(max) (ps)	n_1	n_2
Base	1.4	120	3–4	20	100	200	250	0.1	40	1	1
dNu	1.4	120	10	20	100	200	250	0.1	40	1	1
dA_6	1.5	120	10	40	100	120	140	0.1	6.15	1	1
$(dA)_{12}(dT)_{12}$	2.5	120	19	60	120	140	160	0.1	7.3	1.5	1

TABLE X.
Rate Constants for the Reactions Between Hydrated Electrons and Bases, Monodeoxynucleotides, $(dA)_6$, and $(dA)_{12}(dT)_{12}$.

Molecule	No electrostatic force	With electrostatic forces	Exp.
Bases			
Ade	8.4 ± 0.6	12.6 ± 0.6	9
Cyt	8.1 ± 0.4	10.1 ± 0.4	13
Gua	10.5 ± 0.5	11.0 ± 0.4	
Thy	10.1 ± 0.3	11.2 ± 0.5	18
Ura	10.1 ± 0.6	11.4 ± 0.3	15
Deoxynucleotides			
5′dAMP	9.2 ± 0.5	5.9 ± 0.2	~ 3.8
5′dCMP	8.6 ± 0.4	6.9 ± 0.4	~ 6.8
5′dGMP	9.0 ± 0.4	6.0 ± 0.3	
5′dTMP	8.2 ± 0.5	6.0 ± 0.4	~ 1.5
Poly DA[a]			
5′-$(dA)_6$	3.7 ± 0.1	1.60 ± 0.04	~ 0.25
DNA[a]			
$(dA)_{12}(dT)_{12}$	1.72 ± 0.02	0.26 ± 0.04	0.060–0.14

Rate constants are $10^9\ M^{-1}s^{-1}$. The temperature is 25°C and the ionic strength is 100 m*M*. Experimental rate constants are from Hüttermann et al[13]. The " ~ " signs denote experimentally determined *k* values for the nucleotides, not the deoxynucleotides.
[a]Rates are given per nucleotide base. Error bars are given as 95% confidence limits.

The following conclusions can be drawn by comparing the results from the Brownian dynamics simulations and the corresponding experimental data:

1. The rate constants for the different systems studied are of the correct order of magnitude, except for the six-residue polydeoxynucleotide. Because simulations deliver physically meaningful results for all the other systems, including the highly charged DNA double-helix, it seems probable that the discrepancy between the simulated and experimental results for the polydeoxynucleotide may be attributed to the fact that the experimental rate constant is for poly-A rather than poly-dA, and that the polydeoxynucleotide may be flexible in solution, but was modeled as a rigid molecule in the Brownian dynamics simulations.
2. Within the base series, we have not yet obtained the correct relative magnitudes for the simulated rate constants, although the order of magnitude of each *k* is comparable to the corresponding experimental value. These discrepancies may result from the use of model parameters, such as the diffusion constants of the bases, that are not accurate enough. To distinguish the fine differences of the rate constant among the bases, more accurate simulation parameters need to be used in the model calculations.
3. The "no force" simulation has been performed to demonstrate the effect of absence of electrostatic force on the rate constants. There is no significant difference between the no-force and force cases for the base series. These results are not surprising because the net charges of the bases are zero and the hydrated electrons only feel small electrostatic forces until they are close to the bases. When the hydrated electrons are far away from the bases, their behavior is largely described by an almost random Brownian motion, free from electrostatic steering effects from the bases. the rate constants for the polydeoxynucleotide and the DNA are reduced to a greater extent when the electrostatic interactions are turned on, demonstrating the strong effects of the elecrostatic

repulsive forces between the hydrated electrons and the phosphate groups. These electrostatic effects also partially explain the decrease in the rate constants as one goes from the base series to the highly charged DNA. This trend of decreasing rate constants has previously been attributed to a decrease in the collision frequency of the particle with a given base in a polydeoxynucleotide or DNA[37]. This characteristic has been termed the ''DNA shielding effect'' by Ward et al[38]. In a DNA molecule, for example, each base may experience fewer collisions with hydrated electrons because it is less exposed in a double-helix. In the Brownian dynamics simulations, the effects of electrostatic interactions were accounted for in addition to the exposed surface area effects. Electrostatic interactions further reduced the reaction rate constants due to the strong repulsion between the negative phosphates on the DNA double-helix and the hydrated electrons. Such electrostatic effects on the rate constants have been observed experimentally[38] and asserted theoretically by Greenstock et al[39].

In summary, our simulation show that the hydrated electron reactivity decreases for the bases through the mono- and polydeoxynucleotides, to the DNA. This decrease in reactivity cannot be accounted for solely by a decrease in the exposed area of a base in a polydeoxynucleotide or a DNA double-helix. Although this effect is present, as shown by the no-force simulations, electrostatic repulsive effects from the phosphate groups appear to play an even larger role. It is also interesting to see that the reactive rate constants for the negatively charged deoxynucleotides, 5′$(dA)_6$, and the DNA are all larger than the corresponding experimental values. Because we discussed earlier that the use of a linearized PBE would have overestimated the reactive rate constants, the use of a full PBE would give results closer to the experimental values.

Relative Reactive Probabilities

We have also analyzed the relative probabilities that hydrated electrons attack different sites of the 12-base-pair B-DNA, $dA_{12}dT_{12}$. In calculating the reactive probabilities, the simulations were carried out by including all the reactive sites explicitly. We were not using the approximation that the reactive probabilities of different sites could be obtained by carrying out simulations in which only one site was switched on and putting these results together by assuming that the reactivity of one site was not affected by the reactivity of another. From the simulations including all the reactive sites, we explicitly counted the fraction of trajectories that reacted with each site. Because there are many reactive sites on the 12-base-pair B-DNA, $dA_{12}dT_{12}$, and the electrostatic repulsion between the negatively charged DNA, and the hydrated electron is large (resulting in many trajectories terminated in the outermost surface rather than reacting), one million trajectories were run to obtain good statistics for the analysis discussed here.

For the control, in which the electrostatic forces are turned off, we found that the electrons preferred to attack the two ends of the double-helix (Figure 1a). This is probably because the reactive sites on the ends of the double-helix are more exposed. The results for the A strand and the T strand separately are presented in Figures 1b and 1c, respectively. One can again see that the relative reactive probabilities are higher at the two ends of each strand, and the reactivities of the A and T strands are roughly the same. The reactivity patterns change somewhat when the electrostatic interactions between the DNA and the hydrated electrons were accounted for in the simulation. Figure 1a shows that the reactivities are still higher at the two ends of the double-helix. However, the relative reactivities are higher at the two ends of the helix relative to those in the control, in which all the electrostatic forces are turned off. The reactivities at the center of the helix are also substantially decreased. On the other hand, the third and fourth bases present slightly higher relative reactivities relative to the control. An examination of the electrostatic potential on the molecular surface of the DNA molecule using the graphics program GRASP[40] indicated that the electrostatic potential near the center of the double-helix was much more repulsive against electrons than at the ends of the double-helix, which explained the low reactivities at the center of the helix. This effect is likely to be exaggerated further when the full instead of the linear approximation of the PBE is solved, because the latter approximation overscreened the electrostatic repulsions between hydrated electrons and the centers of the DNA molecules. Figures 1b and

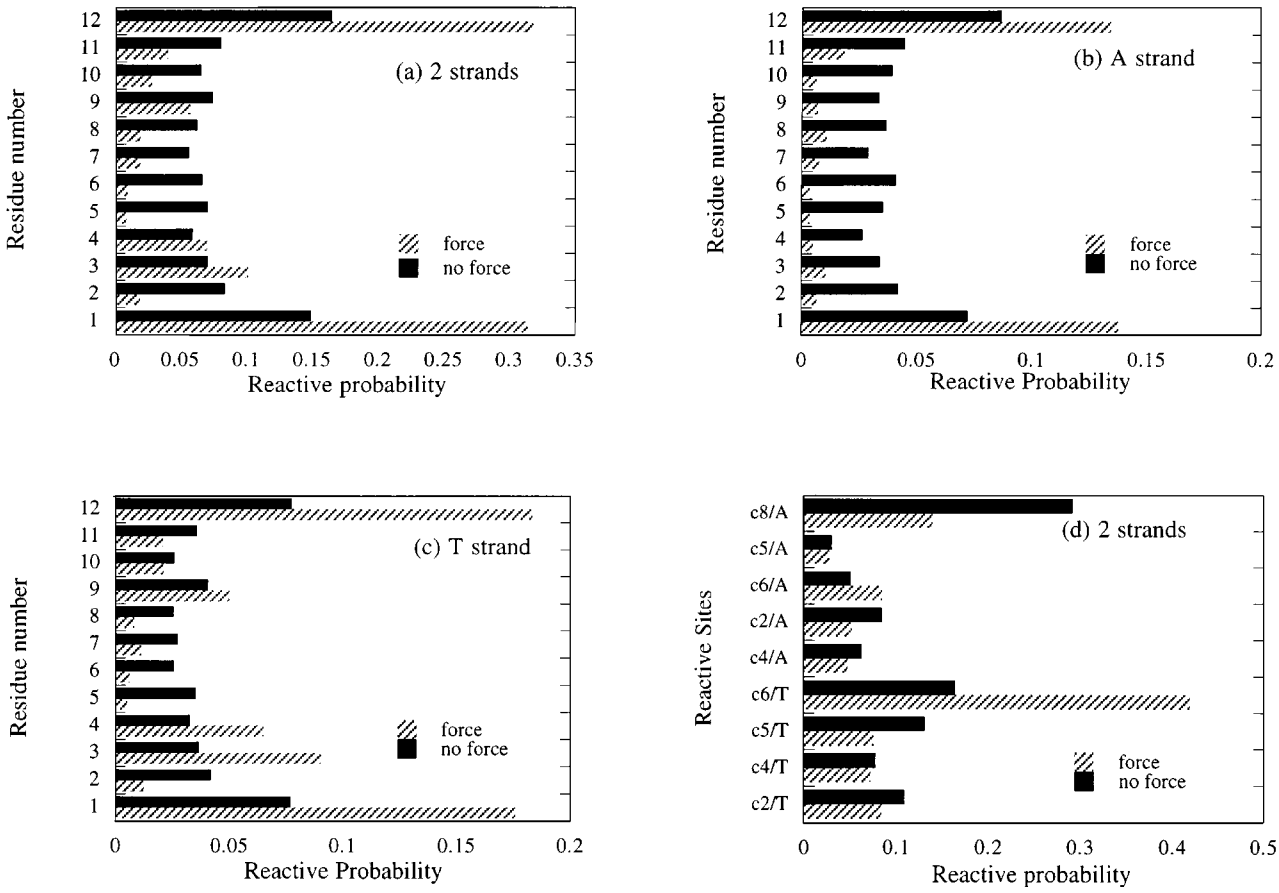

FIGURE 1. The relative reactive probabilities of hydrated electrons to different bases of a $dA_{12}dT_{12}$ double-helix.

1c demonstrate the decomposition of the relative reactive probabilities into the contributions from the A and T strands. By comparing the results of Figures 1a, 1b, and 1c for the case in which electrostatic interactions are turned on, one can see that the overall reactivity patterns shown in Figure 1a are dominated by the contribution from the T strand, which gives relative reactive probabilities about a factor of 2 larger than those from the A strand. This is different from the control in which the two strands have approximately the same reactivities. Figure 1d shows that the preference of hydrated electrons to attack the T strand is due to the substantial increase of the reactivity of the C6 sites of the thymine bases, mostly at the expense of the C8 sites of the adenine bases. This is probably because the charges of the C6 sites of the thymine bases are more positive than those on the C8 sites of the adenine bases, at least for the AMBER potential[27]. The preference of hydrated electrons to attack the C6 site of thymine relative to the C8 sites of adenine will probably be even more pronounced when the full PBE is solved, because the linearized approximation to the PBE appears to overscreen electrostatic interactions.

The reactivities of the C2, C4, C5, and C6 sites of adenine and the C2, C4, and C5 sites of thymine are much less affected by electrostatic interactions, probably because their reactivities are determined to a greater extent by geometric factors. Their smaller exposure makes them less susceptible to attack by hydrated electrons.

These results demonstrate that although geometrical factors seem to be more important in determining the reactivities of buried reactive sites of the adenine and thymine bases, electrostatic interactions between DNA molecules and hydrated electrons do influence the relative reactive probabilities of hydrated electrons to the exposed sites of DNA molecules, and the technique of Brownian dynamic simulation provides a useful tool for quantifying such effects.

Conclusions

To reduce the cpu time required for carrying out the Brownian dynamics simulations described in this article, a variable time-step algorithm was introduced into the UHBD program[23]. A detailed sensitivity analysis of the choice of model and simulation parameters on affecting the reactive rate constants was also performed, leading to a set of ''optimized'' parameters for carrying out the simulations reliably and economically. It is worth pointing out that, although the time steps used in the regions when a diffusing molecule was far away from its target molecule appeared to be large, we carefully checked and confirmed that the use of such large time steps did not affect the simulation rate constants significantly.

These optimized parameters were then used to carry out extensive calculations on the diffusion-controlled rate constants between hydrated electrons and constituents of DNAs. The simulation results for the diffusion reaction rate constants were of the correct order of magnitude when compared with experimental ones.

The Brownian dynamics simulations also allowed examination of the probability that hydrated electrons affect different sites on a DNA double-helix. By comparing the results obtained from the simulations with and without electrostatic forces, it is clear that electrostatic interactions can play an important role in determining the preference of hydrated electrons attacking different sites of a DNA double-helix, although the reactivities of buried sites appeared to be less affected by electrostatic interactions. This study demonstrated that the technique of Brownian dynamics simulation can be a useful quantitative tool for elucidating the indirect mechanism of radiation damage to DNAs. The Brownian dynamics simulation technique will be integrated with quantum chemical calculations to provide a detailed mechanistic study of the reaction between the H and OH radicals and DNAs.

Acknowledgments

The UHBD program was kindly provided by Professsor J. Andrew McCammon. C.F.W. also acknowledges useful discussions with Professor Jeffry D. Madura and Dr. Malcolm E. Davis.

References

1. W. A. Glass and M. N. Varma, Eds., *Physical and Chemical Mechanisms in Molecular Radiation Biology*, Vol. 58, Phenum Press, New York, 1991.
2. I. G. Draganic and Z. D. Draganic, *The Radiation Chemistry of Water*, Academic Press, New York, 1971.
3. C. von Sonntag, *The Chemical Basis of Radiation Biology*, Taylor & Francis, London, 1987.
4. A. J. Bertinchamps, J. Hutterman, W. Kohnlein, and R. Teoule, eds., *Effects of Ionizing Radiation on DNA*, Springer, Berlin, 1978.
5. E. O. Hole, W. H. Nelson, E. Sagsturn, and D. M. Close, *Radiat. Res.*, **129**, 119 (1992).
6. S. Steenken, *Chem. Rev.*, **89**, 503 (1989).
7. G. R. Freeman, Ed., *Kinetics of Nonhomogeneous Processes*, John Wiley & Sons, New York, 1987.
8. D. L. Ermak and J. A. McCammon, *J. Chem. Phys.*, **69**, 1352 (1978).
9. E. Dickinson, *Chem. Sov. Rev.*, **14**, 421 (1985).
10. D. J. Deeble and C. von Sonntag, *Int. J. Radiat. Biol.*, **46**, 247 (1984).
11. D. G. E. Lemaire, E. Bothe, and D. Schulte-Frohlinde, *Int. J. Radiat. Biol.*, **45**, 351 (1987).
12. L. Pardo, J. Banfelder, and R. Osman, *J. Am. Chem. Soc.*, **114**, 2382 (1992).
13. A. J. Bertinchamps, J. Hüttermann, W. Köhlein, R. Téoule, Eds., *Effects of Ionizing Radiation on DNA*: *Physical*, *Chemical* & *Biological Aspects*, Springer, New York, 1978.
14. S. H. Northrup, S. A. Allison, and J. A. McCammon, *J. Chem. Phys.*, **80**, 1517 (1984).
15. M. E. Davis and McCammon, *J. Comput. Chem.*, **10**, 386 (1989).
16. M. K. Gilson, K. A. Sharp, and B. H. Honig, *J. Comput. Chem.*, **9**, 327 (1987).
17. M. K. Gilson and B. H. Honig, *Nature*, **330**, 84 (1987).
18. B. Jayaram, K. A. Sharp, and B. Honig, *Biopolymers*, **28**, 975 (1989).
19. I. Klapper, R. Hagstrom, R. Fine, K. Sharp, and B. Honig, *Proteins*, **1**, 47 (1986).
20. A. Nicholls and B. Honig, *J. Comput. Chem.*, **12**, 435 (1991).
21. K. Sharp and B. Honig, *Annu. Rev. Biophys. Chem.*, **19**, 301 (1990).
22. J. Warwicker and H. C. Watson, *J. Mol. Biol.*, **157**, 671 (1982).
23. B. A. Luty, et al., UHBD, Houston, Tx (1990).
24. S. H. Northrup and J. T. Hynes, *J. Chem. Phys.*, **71**, 871 (1979).
25. M. S. Inc., QUANTA, Waltham, MA, 1990.
26. B. R. Brooks, et al., *J. Comput. Chem.*, **4**, 187 (1983).
27. S. J. Weiner, et al., *J. Am. Chem. Soc.*, **106**, 765 (1984).
28. J. D. Dwyer and V. A. Bloomfield, *Biophys. J.* **65**, 1810 (1993).
29. W. Yu, C. F. Wong, and J. Zhang, *J. Phys. Chem.* (in press)

30. E. Hayon, *J. Chem. Phys.*, **51**, 4881 (1969).
31. A. Kamal and W. M. Garrison, *Nature*, **206**, 1315 (1965).
32. R. A. Holroyd and J. W. Glass, *Int. J. Radiat. Biol.*, **14**, 445 (1968).
33. A. D. Lenherr and M. G. Ormerod, *Nature* **225**, 546 (1970).
34. E. J. Hart and M. Anbar, *The Hydrated Electron*, John Wiley & Sons, New York, 1970.
35. W. J. Bowen and H. L. Martin, *Arch. Biochem. Biophys.*, **107**, 30 (1964).
36. M. M. Tirado, C. L. Martinez, and J. Garcia de la Torre, *J. Chem. Phys.*, **81**, 2047 (1984).
37. P. C. Shragge, H. B. Michaels, and J. W. Hunt, *Radiat. Res.*, **47**, 598 (1971).
38. J. F. Ward, *Advances in Radiation Biology*, Vol. 5, 1975, p. 181.
39. C. L. Greenstock, M. Ng, and J. Hunt, *Advan. Chem. Ser.*, **81**, 397 (1968).
40. A. Nicholl, GRASP, Columbia University, New York.